Mössbauer spectroscopy of synthetic and naturally occurring staurolite

M. Darby Dyar, Chryl L. Perry, Carolyn R. Rebbert

Department of Geological Sciences, University of Oregon, Eugene, Oregon 97403, U.S.A.

Barbara L. Dutrow

Department of Geology and Geophysics, Louisiana State University, Baton Rouge, Louisiana 70803, U.S.A.

Michael J. Holdaway

Department of Geological Sciences, Southern Methodist University, Dallas, Texas 75275, U.S.A.

Helen M. Lang

Department of Geology and Geography, West Virginia University, Morgantown, West Virginia 26506, U.S.A.

Abstract

Room temperature Mössbauer spectroscopic measurements of 23 natural and 12 synthetic staurolite samples, the latter representing both Fe-Mg and Fe-Li solutions, demonstrate that the majority of the Fe in all samples is Fe^{2+} which occupies the Fe1, Fe2, and Fe3 subsites of the tetrahedral Fe site in an average ratio of 43/12/27. This model is consistent with the H content of the samples where it is known. Additional Fe^{2+} occupancy averaging 11% of Fe_{tot} in the sample occurs in some combination of the Al(3A), Al(3B), U(1), and U(2) octahedral sites. Some $^{[4]}Fe^{3+}$ (averaging 5% in natural and 8% in synthetic samples) is also present, probably replacing Al in the Si site. A poorly resolved doublet with a mean isomer shift of 0.89 mm/s (9% of Fe_{tot}), possibly representing a charge transfer doublet, is also observed in approximately half the samples. Mössbauer parameters of the various sites do not vary systematically with composition and appear to be independent of next nearest neighbor effects (except in the case of H). These results corroborate previous structure refinement data on the existence of three major Fe subsites and provide direct evidence of minor Fe occupancy in the octahedral sites.

Introduction

The mineral staurolite has long maintained its reputation as a crystal chemical puzzle. Much of the difficulty lies in accurately determining the locations and amounts of different atomic species within the crystal structure. The basic structure as determined by Náray-Szabó (1929), Hurst et al. (1956), and Smith (1968) consists essentially of layers of kyanite composition alternating with iron aluminum hydroxide monolayers along the **b** crystallographic direction. It has been well established (e.g., Smith, 1968; Griffen and Ribbe, 1973; Holdaway et al., 1986b; Ståhl et al., 1988) that the composition of the kyanite layer is essentially pure Al_2SiO_5 and that the sites are fully occupied. However, within the monolayer, numerous sites are available for cation substitutions and are characteristically only partially occupied (Smith, 1968; Takéuchi et al., 1972). One unit cell contains two each of the octahedrally coordinated Al(3A), Al(3B), U(1), and U(2) sites, four of the tetrahedrally coordinated Fe sites, and four each of the proton sites P(1A), P(1B), H(2A), and H(2B) (Fig. 1). The P and H designations for the H sites are used interchangeably. For simplicity we propose abandonment of the H nomenclature from the literature (the P designation has historical precedence) by renaming of the H(2A) and H(2B) sites to P(2A) and P(2B), respectively; this convention will be used here. Also note that the nomenclature for crystallographic sites follows the conventions established by Smith (1968).

No one analytical method can uniquely determine cation site assignments; rather, the results of different techniques must be brought to bear in unravelling the crystal chemistry of staurolite. For example, the similarity in X-ray scattering factors for Mg and Al makes separate site assignments of these species ambiguous (Smith, 1968). A similar difficulty exists in distinguishing between Mg and $Li_{0.5}Fe_{0.5}$ for both X-ray and neutron diffraction experiments (Ståhl et al., 1988). H contents are often not determined, yet the presence of H has been postulated to affect the occupancy of both the Fe site (Takéuchi et al., 1972; Holdaway et al., 1986b) and the Al(3) site (Donnay and Donnay, 1983; Holdaway et al., 1986b). Neutron diffraction studies have located the protons at the four sites mentioned above (Takéuchi et al., 1972; Ståhl et al., 1988). Li and Zn contents are also often not determined, although they may be important constituents of staurolite (Dutrow et al., 1986; Holdaway et al., 1986b). Minor elements such as Ti, Mn, Co, and Cr occur in such small quantities that they can be assigned to a number of different sites without producing a significant difference from the observed X-ray electron densities (Ståhl et al., 1988).
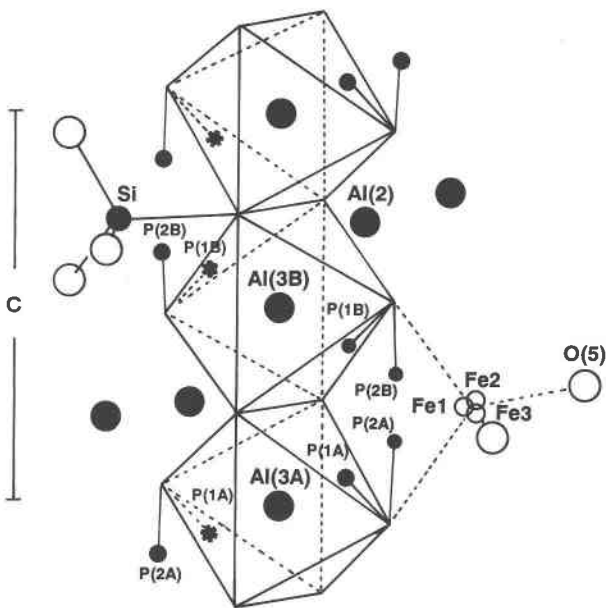
Fig. 1. The positions of Fe1, Fe2, and Fe3 subsites with respect to the H sites are shown here along with the Al(3A) and Al(3B) sites (after Takéuchi, 1972). The atomic coordinates of the Fe subsites were determined by Alexander (1989) to be (0.3778,0,0.2497), (0.4027,0,0.2783), and (0.3994,0,0.2291) for Fe1, Fe2, and Fe3, respectively. Note that the Fe1 site, which is occupied by Fe^{2+} when the P sites are unoccupied, is (therefore) the closest to those sites. Occupancies of P(2A) and P(2B) are low relative to P(1A) and P(1B) (Tagai and Joswig, 1985).

To determine site occupancies of minor elements, other methods such as optical spectroscopy (Ward, 1984) and synthesis of staurolite rich in minor elements (e.g., Phillips and Griffen, 1986) must be employed.

Fe also poses problems for assignment to specific sites. Numerous Mössbauer studies of staurolite are internally consistent (Table 1), but the interpretation of the spectra and assignment of the doublets to particular cation sites is debatable. Bancroft et al. (1967), Smith (1968), Regnard (1976), and Phillips and Griffen (1986) all consider the majority of the Fe^{2+} to be in the tetrahedral Fe site with approximately 25–40% in two or more octahedral sites. The isomer shifts (*IS*) ($\delta = 0.92$–1.05 mm/s) and quadrupole splittings (*QS*) ($\Delta = 1.03$–1.53 mm/s) reported as octahedral tend to be low for sixfold coordination, but Bancroft et al. (1967) noted that the octahedral Al(3) sites are very distorted. Such distortions tend to decrease the values of the Mössbauer parameters. Smith (1968) demonstrated that such an assignment is reasonable based on the interatomic distances and population factors of his X-ray structure refinement. Phillips and Griffen (1986) found these parameters to be comparable to those for $^{[6]}Fe^{2+}$ in an ilvaite ($\delta = 0.95$ and 1.15 mm/s).

Alternatively, Dowty (1972) assigned both doublets observed in his samples to $^{[4]}Fe^{2+}$, because the *IS*, which do not differ appreciably, are both typical of fourfold coordination. Although the staurolite crystal structure con-

tains only one tetrahedral Fe site, he suggested that the occurrence of more than one tetrahedral ferrous doublet must be the result of Fe atoms arrayed among the three centers of displacement of the Fe site as described by Smith (1968). Likewise, Alexander (1989), who completed an X-ray and Mössbauer study of a natural staurolite, confirmed the presence of at least three Fe subsites to which she assigned three of her resolved doublets. In accord with the ideas of Holdaway et al. (1986b) and Ståhl et al. (1988), Alexander (1989) ascribed the presence of three Fe subsites to interactions between Fe^{2+} and H^+. The most populated site, Fe1, is closer to the Al(3) octahedral chain, because both P(1A) and P(1B) are vacant. The Fe3 site is the next most populated site and corresponds to the presence of a proton at P(1B). Fe2, the least populated site, is associated with a proton at P(1A) (Fig. 1).

Temperature dependence of the inner doublets has been used to support as many different interpretations as workers who have noted it (Dowty, 1972; Regnard, 1976; Scorzelli et al., 1976; Sharma et al., 1987; Alexander, 1989). Dowty (1972), employing the work of Gibb (1968), noted that such a temperature dependence is not anticipated for distorted $^{[6]}Fe^{2+}$ but is consistent for $^{[4]}Fe^{2+}$. Scorzelli et al. (1976) agreed that a permanently distorted octahedral site should not show such variations in *QS* with temperature. However, they calculated an activation energy for the process which is on the order of those for electron transfer mechanisms. They further argued that the decreased intensity of the inner doublet with decreasing temperature is the result of an actual disappearance of that doublet due to a decreasing rate of electron exchange and the subsequent localization of the electron at an anion vacancy. Phillips and Griffen (1986) disagreed with both of the above studies and noted that the changes in the Mössbauer parameters with temperature of $^{[6]}Fe^{2+}$ in ilvaite are similar to those observed by Dowty (1972) and are therefore consistent with $^{[6]}Fe^{2+}$ in staurolite. On the basis of recoil-free factors calculated from the temperature dependence of their two ferrous doublets, Sharma et al. (1987) concluded that their inner doublet is the result of an impurity and therefore all the Fe^{2+} is in one tetrahedral site. Alexander (1989) observed, however, that the shifts which result from temperature changes are within the errors she cited for peak positions and so are not a reliable basis on which to propose assignments.

A few studies reported the possible presence of Fe^{3+} and estimated that it composes 2–5% of Fe_{tot} in staurolite (Dowty, 1972; Regnard, 1976; Phillips and Griffen, 1986). Varma and Varma (1987) interpreted two of their four doublets as the result of $^{[6]}Fe^{3+}$, but gave no basis for the assignment. Sharma et al. (1987) assumed that the ferric doublet which accounts for 6% of the total spectrum area is the result of an impurity. Alexander (1989) assigned her fourth doublet to $^{[6]}Fe^{3+}$ based on an *IS* of 0.60 mm/s, but from her published spectrum the *IS* appears to be closer to 0.20 mm/s and thus corresponds to $^{[4]}Fe^{3+}$.

The purpose of this study is to clarify the site assign-

TABLE 1. Previous Mössbauer studies of staurolite

Reference	Site 1		Site 2		Site 3		Site 4	
	IS	QS assignment	IS	QS assignment	IS	QS assignment	IS	QS assignment
Bancroft et al., 1967	0.97	2.30 $^{[4]}Fe^{2+}$	1.05	1.30 $^{[6]}Fe^{2+}$	—	—	—	—
	0.97	2.29 $^{[4]}Fe^{2+}$	1.01	1.25 $^{[6]}Fe^{2+}$	—	—	—	—
Smith, 1968	0.97	2.33 $^{[4]}Fe^{2+}$	0.99	1.53 $^{[6]}Fe^{2+}$ (Al3, U)	—	—	—	—
Dowty, 1972	0.95	2.30 $^{[4]}Fe^{2+}$	1.03	1.30 $^{[4]}Fe^{2+}$	—	—	—	—
	0.95	2.29 $^{[4]}Fe^{2+}$	0.99	1.25 $^{[4]}Fe^{2+}$	—	—	—	—
	0.96	2.33 $^{[4]}Fe^{2+}$	0.98	1.53 $^{[4]}Fe^{2+}$	—	—	—	—
	0.97	2.35 $^{[4]}Fe^{2+}$	0.99	1.56 $^{[4]}Fe^{2+}$	—	—	—	—
Takéuchi et al., 1972	1.21	2.41 $^{[4]}Fe^{2+}$	—	—	—	—	—	—
Scorzelli et al., 1976	0.93	2.23 $^{[4]}Fe^{2+}$	0.94	1.25 CT Fe^{2+}	—	—	—	—
Regnard, 1976	0.94	2.38 $^{[4]}Fe^{2+}$	0.95	1.80 $^{[6]}Fe^{2+}$ (Al3)	0.92	1.03 $^{[6]}Fe^{2+}$ (Al3)	—	—
Dzhemai, 19788a	0.99	2.49	0.97	1.50	1.08	0.70	—	—
Dzhemai, 1978b	0.86	2.27	0.88	1.85	0.84	1.37	0.87	0.83
	0.86	2.31	0.88	1.91	0.87	1.28	0.90	0.71
	0.86	2.51	0.86	2.16	1.25	1.52	0.83	0.88
	0.88	2.38	0.89	2.05	0.86	1.34	0.90	0.72
	0.89	2.52	0.90	2.25	0.92	1.66	0.96	0.77
	0.89	2.44	0.90	2.12	0.90	1.29	0.93	0.63
	0.90	2.47	0.90	2.21	0.94	1.84	0.97	0.93
	0.92	2.57	0.93	2.21	0.95	1.64	0.96	0.74
	0.92	2.40	0.96	1.96	0.93	1.18	0.90	0.80
	0.93	2.53	0.94	2.23	0.96	1.76	1.02	0.84
	0.93	2.50	0.94	2.20	0.92	1.69	0.94	0.91
	0.93	2.49	0.93	2.21	0.95	1.70	0.99	0.80
	0.93	2.45	0.93	2.13	0.91	1.33	0.96	0.74
	0.99	2.49	0.99	2.13	0.97	1.50	1.08	0.76
	1.02	2.50	1.01	2.05	1.00	1.39	1.01	0.72
Phillips and Griffen, 1986	0.97	2.35 $^{[4]}Fe^{2+}$	1.05	1.20 $^{[6]}Fe^{2+}$ (Al3, U)	—	—	—	—
Varma and Varma, 1987	1.02	2.18 $^{[4]}Fe^{2+}$	0.98	1.63 $^{[6]/[4]}Fe^{2+}$	1.11	0.68 $^{[6]}Fe^{3+}$	0.16	0.58 $^{[6]}Fe^{3+}$
	1.05	2.11 $^{[4]}Fe^{2+}$	1.04	1.63 $^{[6]/[4]}Fe^{2+}$	1.16	0.68 $^{[6]}Fe^{3+}$	0.20	0.63 $^{[6]}Fe^{3+}$
	1.03	2.16 $^{[4]}Fe^{2+}$	0.97	1.66 $^{[6]/[4]}Fe^{2+}$	1.14	0.69 $^{[6]}Fe^{3+}$	0.18	0.58 $^{[6]}Fe^{3+}$
	1.08	2.02 $^{[4]}Fe^{2+}$	1.04	1.48 $^{[6]/[4]}Fe^{2+}$	1.12	0.65 $^{[6]}Fe^{3+}$	0.23	0.66 $^{[6]}Fe^{3+}$
Sharma et al., 1987	0.98	2.34 $^{[4]}Fe^{2+}$	0.97	1.31 Fe^{2+} impurity	—	—	0.18	1.05 Fe^{3+} impurity
	0.96	2.38 $^{[4]}Fe^{2+}$	0.85	1.53 Fe^{2+} impurity	—	—	0.21	0.91 Fe^{3+} impurity
Alexander, 1989	0.96	2.50 $^{[4]}Fe^{2+}$ (Fe2)	0.98	2.13 $^{[4]}Fe^{2+}$ (Fe1)	0.92	1.17 $^{[4]}Fe^{2+}$ (Fe3)	0.60	0.83 $^{[6]}Fe^{3+}$ (Al3)

ments and occupancies of Fe in staurolite. We will show that the study of a wide compositional range of samples at a single (room) temperature clarifies peak assignments in a way in which variable temperature studies of single specimens cannot.

METHODS

Samples

Mössbauer spectroscopic measurements have been made on a suite comprising 12 synthetic and 23 natural staurolite samples (Table 2). These included a series of five Fe-Mg (Rice, 1985) and seven Fe-Li synthetic staurolite solutions (Dutrow, 1991), four natural staurolite samples from a site at Hunt Valley, Maryland (Lang, 1986), and 19 samples included in or relating to earlier studies (Holdaway et al., 1986a, 1986b). Some of the latter samples were provided by Douglas Rumble, III and by Jeffrey Grambling. Information on locality and assemblage, and references for these and other staurolite samples included in this study are summarized in Table 2.

Natural mineral separates were prepared by crushing and sieving the rocks to 100–325 mesh or ≤325 mesh, followed by repeated elutriation to remove dust and fines. Samples prepared at Southern Methodist University (SMU) were centrifuged with methylene iodide to remove minerals with density ≤3.3, followed by separation with a Frantz isodynamic separator. Samples prepared at the University of Oregon were also magnetically separated, followed by hand picking to remove impurities. Natural samples are therefore estimated to be better than 97.5% pure. The products of synthesis experiments were checked for yield using refractive oils and are estimated to be at least as pure as the natural separates. Mössbauer analysis found no trace of Fe-bearing impurities in any natural or synthetic samples (detection limit is 1% of Fe_{tot} in a sample).

Microprobe analyses

Microprobe analyses (Table 3) of the natural samples were obtained using an automated JEOL-733 microprobe

TABLE 2. Localities, synthesis conditions, and assemblages for staurolite specimens

	Locality	Assemblage + Qtz (except EH-6)*	Reference or source	Comments
356-1	Bashbish Falls, Connecticut	Bt + Gt + Chl + Pl + Ep + Ilm + Mg + Gr + Ms	Zen (1981)	~3H
EH-6	Emery Hill, New York	Bt + Gt + Chl + Ged + Cum + Sil + Crn + Mag	Tracy	~3H
B14040	Pizzo Forno, Switzerland	Bt + Pg + Ky + Ms	Smithsonian	~3H
117189	Stratford, North Carolina	Nearly pure St, Gah + Ms	Smithsonian	~3H, high Zn
6-3	East Winthrop, Maine	Bt + Gt + Sil + Pl + Ilm + Ms	Holdaway	~3H, high Li
3-3	West Sidney, Maine	Bt + Gt + Chl + Crd + And + Ilm + Ms	Osberg (1971)	~3H
114-1	Byron, Maine	Bt + Gt + Chl + Ilm + Gr + Ms	Holdaway	~3H, high Li
53-2	East Dixfield, Maine	Bt + Gt + Sil + Ilm + Gr + Ms	Holdaway	~3H
ER-70	Errol quad, New Hampshire	Bt + Gt + Ilm + Ms	Green (1963)	~3H
117183	Fannin County, Georgia	Nearly pure St, Bt + Ms	Smithsonian	~3H
82TP9	Truchas Mountains, New Mexico	Bt + Hem + And + Gt + Ms	Grambling	~3H, high Zn
82TP9A	Truchas Mountains, New Mexico	Bt + Hem + And + Gt + Ms	Grambling	~3H
203	Embden, Maine	Bt + Gt + Ilm + And + Ms + Gr	Holdaway	~3H
HV-4	Hunt Valley, Maryland	Bt + Mag + Gt + IlmHem + Chl + Ms + Pl	Lang	~3H
HV-10	Hunt Valley, Maryland	Bt + Po + Gt + Ilm + Ms + Pl	Lang	~3H
HV-112	Hunt Valley, Maryland	Bt + Mag + Gt + IlmHem + Ms + Pl	Lang	~3H
HV-116	Hunt Valley, Maryland	Bt + Mag + Gt + IlmHem + Ms + Pl	Lang	~3H
77-55C	Truchas Mountains, New Mexico	And + IlmHem + Ms	Grambling	~4H, high Li
71-60E	Black Mountain, New Hampshire	Chl + Cld + IlmHem + Mag + Ms	Rumble (1978)	~4H
71-62R	Black Mountain, New Hampshire	Chl + Cld + IlmHem + Mag + Ms	Rumble (1978)	~4H
71-62U	Black Mountain, New Hampshire	Chl + Cld + Ky + IlmHem + Mag + Ms	Rumble (1978)	~4H
71-62T	Black Mountain, New Hampshire	Chl + Cld + Ky + IlmHem + Mag + Ms	Rumble (1978)	~4H
71-62B	Black Mountain, New Hampshire	Cld + Ky + IlmHem + Mag + Ms	Rumble (1978)	~4H
		Synthesis conditions		
Fe100	U.B.C.	15Kb, 720C, graphite furnace	Rice	Fe:Mg = 100:0
Fe90	U.B.C.	15Kb, 720C, graphite furnace	Rice	Fe:Mg = 90:10
Fe80	U.B.C.	15Kb, 730C, graphite furnace	Rice	Fe:Mg = 80:20
Fe70	U.B.C.	15Kb, 720C, graphite furnace	Rice	Fe:Mg = 70:30
Fe60	U.B.C.	15Kb, 720C, graphite furnace	Rice	Fe:Mg = 60:40
FeLi-40-2	F.R.G.	15Kb, 720C, FMQ	Dutrow	Fe:Li:Al:Si = 4.0:0.0:18.0:7.5
FeLi-40-4	F.R.G.	30Kb, 720C, IW	Dutrow	Fe:Li:Al:Si = 4.0:0.0:18.0:7.5
FeLi-35-3	F.R.G.	30Kb, 720C, IW	Dutrow	Fe:Li:Al:Si = 3.5:0.5:18.08:7.5
LiAl-25-1	F.R.G.	30Kb, 720C, IW	Dutrow	Fe:Li:Al:Si = 2.5:1.5:17.93:8.0
FeMg-22-2	F.R.G.	30Kb, 720C, FMQ	Dutrow	Fe:Mg:Al:Si = 2.0:2.0:18.0:7.5
FeLi-225-1	F.R.G.	30Kb, 720C, IW	Dutrow	Fe:Li:Al:Si = 2.2:1.7:18.58:7.5
LiAl-767-2	F.R.G.	30Kb, 720C, IW	Dutrow	Fe:Li:Al:Si = 3.0:1.0:17.767:8.0

Note: U.B.C. and F.R.G indicate that the staurolite samples were synthesized at the University of British Columbia and the Ruhr Universität, Bochum, Germany. IW = iron-wüstite buffer; FMQ = fayalite-magnetite-quartz buffer.
* IlmHem = hematite-bearing ilmenite.

at SMU and methods described in Holdaway et al. (1986b). Microprobe analyses were not available for the synthetic staurolite samples because of analytical difficulties related to their small grain size. Starting compositions are listed in Table 2.

Mössbauer analyses

Samples were mixed with sugar by hand under acetone (to minimize possible oxidation of Fe) to insure a random, thin distribution of sample within the holder. Initial sample quantities of synthetic samples were low (approximately 20–30 mg, in contrast with the 150–300 mg used in the mounts of natural samples) making measurement of high quality Mössbauer spectra difficult. Thus, spectral fits for the synthetic samples have generally higher errors. Nevertheless, the Fe content in the sample mounts of synthetic staurolite corresponds to about 0.4–0.8 mg FeO/cm² (compared with an ideal value of 7 mg FeO/cm²; see Dyar, 1984 for details) which does yield statistically acceptable data if data are collected over a long period.

Mössbauer measurements were recorded in 1024 channels of a constant acceleration Austin Science Associates spectrometer (Dyar et al., 1989). A source of 50–30 mCi ^{57}Co in Pd was used; results were calibrated against α-Fe foil of 6 μm thickness and 99.99% purity. The program Stone (Stone et al., 1984) was used to fit the spectra on personal computers. This program uses a Gaussian non-linear regression procedure with the capability to constrain any set of parameters. Lorentzian line shapes were used for resolving peaks. This assumption was tested on two different spectra by fitting with peaks of increasing percentages of Gaussian component. No improvement in the statistics of those fits was observed within the known errors of the technique, nor was any significant change in peak areas noted. Therefore the addition of a Gaussian component to peak shapes was not utilized subsequently. Results are summarized in Table 4.

Initial fits of the staurolite spectra, in which two Fe^{2+} doublets were fit with peak positions unconstrained and widths and areas constrained in pairs, resulted in Möss-

bauer parameters similar to those of Bancroft et al. (1967). However, a broad inner doublet and an unsatisfactory χ^2 value seemed to indicate the presence of more than these two doublets (Fig. 2). For these reasons, and because some previous workers have been successful in resolving three (Regnard, 1976) and recently four (Varma and Varma, 1987; Alexander, 1989) doublets in staurolite spectra, successive fits were resolved with three and then four doublets. In spectra with a distribution of peak areas requiring additional peaks in the low velocity regions, estimated peak positions corresponding to Fe^{3+} were introduced into the fitting procedure. Because peak overlap with respect to the Fe^{3+} doublets was often quite pronounced, attempts were made to fit several spectra both with and without Fe^{3+} in order to confirm or refute its presence. In all cases where this test was attempted, individual spectra could be fit only with or without an Fe^{3+} doublet, not both ways. It is therefore extremely unlikely that the Fe^{3+} doublet is an artifact of the method or the fitting procedure.

As additional doublets were added, the overall appearance of the fits (Fig. 2), as well as the values for the χ^2 and misfit parameters (Table 5), continued to improve but were still not entirely satisfactory. For this reason, five doublet fits were attempted. The five doublet fits initially converged only with all peak positions constrained, but as these constraints were gradually released, statistical parameters improved. Final five doublet fits have all peak widths constrained to be equal to one another and areas constrained in pairs; all peak positions are unconstrained (Fig. 2). Because of the heavily overlapped nature of the doublets, it was not possible to obtain converged fits with fewer constraints on widths and areas.

Error analysis is particularly important to this study because of the multiple, heavily overlapped peaks in these complicated spectra. The precision of Mössbauer measurements has been examined using both synthetic (Dollase, 1975) and experimental (Dyar, 1984) data. The former approach evaluates the statistical quality of a given peak parameter based on the formula

$$2\text{Area}/\pi\sqrt{(\text{Baseline} \times \text{Width})},$$

where peak area and width are given in channel numbers. Use of this formulation, which assumes that all peaks in a spectrum are isolated, yields the errors tabulated in the top half of Table 6 for spectra typical of both natural and synthetic samples. For good quality spectra with isolated peaks, these error estimates are generally smaller than the experimentally determined errors found by Dyar (1984). Using replicate analyses of a single standard sample of grunerite with slightly overlapping peaks, she found reproducibilities of ±0.02 mm/s for peak positions, ±0.02 mm/s for widths, and $\pm1.6\%$ of the total area for peak areas. Note that these measurements are standard deviations in the units of measurement and not percentage errors as are given in Table 6.

Additional error is introduced into the peak area data, however, by the overlap of the peaks in the spectra. Dol-

lase (1975) provided a method for estimating the effect of peak overlap on errors in parameter determination. These calculations have been performed on the same two spectra treated above. Table 6 shows the increased errors which are introduced as a result of peak overlap. In this study, good quality data could be obtained only for the natural samples for which sufficient specimen quantities were available. In the spectra of the natural samples, peaks that are not heavily overlapped (e.g., those at the high velocity end of the spectra) have errors roughly comparable to those for isolated peaks as would be expected. Overlapped peaks have slightly higher errors for good quality data, and considerably higher errors in the lower quality spectra of synthetic samples. However, it is gratifying to note that the variances about the mean values of Mössbauer parameters for both the natural and synthetic samples are extremely small (Table 4). Considering that peak positions have not been constrained, such consistency is remarkable. Standard deviations for IS (δ) and QS (Δ) range from 0.01 to 0.07 mm/s for δ and 0.06 to 0.20 mm/s for Δ. These errors are probably reasonable estimates for application to synthetic staurolite spectra; smaller standard errors of ±0.03–0.05 mm/s should be used for spectra of natural staurolite. In summary, the Mössbauer parameters obtained by this study have a high degree of reproducibility although the respective peak areas have the greatest inherent error.

RESULTS

Peak parameters

All spectra were fit with five doublets which represent six distinct sites. Peak parameters of all spectra are summarized in Table 4; typical spectra are shown in Figures 3, 4, and 5. Doublets 1, 2, and 3 are characterized by similar (Fe^{2+}) average IS of $\delta = 0.98 \pm 0.01$, 0.98 ± 0.01, and 0.97 ± 0.02 mm/s respectively, and different average QS ($\Delta = 2.45 \pm 0.06$, 2.10 ± 0.09, and 1.6 ± 0.2 mm/s). A disproportionate amount of the variation in these parameters is contributed by the spectra of Fe-Li synthetic staurolite samples which have the highest errors because of small sample quantities. Relative areas for these three doublets decrease from doublet 1 to doublets 2 and 3 with average relative areas of $43 \pm 7\%$, $27 \pm 5\%$, and $12 \pm 3\%$, respectively.

A fourth doublet with $\delta = 1.07 \pm 0.07$ mm/s and $\Delta = 0.8 \pm 0.1$ mm/s also corresponds to Fe^{2+} and will be referred to as doublet 4. Its average relative area is $11 \pm 2\%$. Doublet 5, which represents Fe^{3+} in these samples, has average $\delta = 0.10 \pm 0.04$ mm/s and $\Delta = 0.7 \pm 0.2$ mm/s, with an average relative area of $7 \pm 3\%$. It is difficult to assign a particular Fe species and site in the staurolite structure to doublet 6 (see Discussion), which has a $\delta = 0.89 \pm 0.04$ mm/s and $\Delta = 0.93 \pm 0.06$ mm/s and an average relative area of $9 \pm 1\%$. Those spectra which have Fe occupancy in doublet 5 (Fe^{3+}) show no Fe occupancy in doublet 6 and vice versa; this mutual exclusivity may be a consequence of overlap of these small peaks.

TABLE 3. Cations per formula unit

Sample	356-1	EH-6	B14040	117189	6-3	3-3	114-1	53-2
Si	7.712	7.590	7.664	7.730	7.806	7.623	7.617	7.493
Al	17.680	17.484	17.563	17.732	17.854	17.868	17.873	17.966
Ti	0.110	0.099	0.127	0.112	0.083	0.114	0.093	0.105
Cr	0.011	0.013	0.009	0.013	0.022	0.020	0.011	0.0187
V	0.006	0.006	0.007	0.007	0.005	0.006	0.009	0.007
Co	0.007	0.007	0.004	0.005	0.004	0.004	0.007	0.004
Fe(1–3)	2.731	2.199	2.350	1.732	2.058	2.558	2.626	2.661
Fe4	0.268	0.353	0.293	0.271	0.248	0.319	0.328	0.337
Fe5	0.100	0.353	0.088	0.084	0.125	0.095	0.098	0.100
Fe6	0.337	0.087	0.293	0.062	0.075	0.319	0.328	0.337
Fe^{2+}	3.340	2.639	2.936	2.065	2.379	3.197	3.282	3.334
Fe^{3+}	0.100	0.353	0.088	0.084	0.125	0.095	0.098	0.100
ΣFe	3.440	2.992	3.024	2.149	2.504	3.292	3.380	3.434
Mg	0.691	1.676	0.926	0.810	0.373	0.789	0.560	0.608
Mn	0.012	0.026	0.049	0.036	0.100	0.114	0.017	0.054
Zn	0.048	0.062	0.059	1.316	0.201	0.037	0.060	0.050
Li	0.124	0.011	0.067	0.057	0.996	0.124	0.417	0.258
H*	2.996	2.836	3.294	3.097	3.304	2.670	2.900	2.962

Sample	77-55C	71-60E	71-62R	71-62U	71-62T	71-62B	FE100	FE90
Si	7.563	7.683	7.670	7.607	7.594	7.592	8.000	8.000
Al	18.033	17.880	17.873	17.900	17.775	18.030	18.000	18.000
Ti	0.072	0.089	0.089	0.084	0.090	0.084	0.000	0.000
Cr	0.000	0.015	0.011	0.000	0.000	0.000	0.000	0.000
V	0.000	0.004	0.007	0.000	0.000	0.000	0.000	0.000
Co	0.000	0.009	0.007	0.000	0.000	0.000	0.000	0.000
Fe(1–3)	2.479	2.291	2.301	2.333	2.372	2.421	3.224	2.830
Fe4	0.333	0.289	0.317	0.288	0.297	0.390	0.388	0.385
Fe5	0.212	0.085	0.086	0.086	0.088	0.091	0.272	0.277
Fe6	0.090	0.231	0.258	0.249	0.266	0.212	0.116	0.104
Fe^{2+}	2.902	2.837	2.875	2.883	2.937	3.025	3.728	3.323
Fe^{3+}	0.212	0.085	0.086	0.086	0.088	0.091	0.272	0.277
ΣFe	3.114	2.922	2.961	2.699	3.025	3.116	4.000	3.600
Mg	0.073	0.326	0.284	0.449	0.465	0.350	0.000	0.400
Mn	0.028	0.080	0.054	0.052	0.056	0.038	0.000	0.000
Zn	0.006	0.018	0.049	0.037	0.026	0.025	0.000	0.000
Li	0.617	0.267	0.322	0.156	0.144	0.067	0.000	0.000
H*	4.090	4.148	4.159	4.283	4.562	3.993		

Note: Stoichiometry is based on 48 O atoms, except where H was not determined. For those analyses, stoichiometry was based on Si + Al + Fe^{3+} + 2Ti/3 − Li/3 = 25.57, and H, shown in parentheses, was estimated by subtracting the charge of the other ions from 96, leading to a 2 σ error of 0.8 ions in H. Fe(1–3), Fe4, Fe5, and Fe6 refer to the proportion of Fe consistent with Fe doublets in the Mössbauer spectra, designated 1–6 in the text.

Peak widths for all doublets in all spectra average 0.31 ± 0.03 mm/s and range from 0.25 to 0.40 mm/s. Because peak widths were constrained to be equal for all five doublets, no conclusions can be drawn regarding widths of individual doublets.

DISCUSSION

Interpretation of the Mössbauer data presented in this study necessitates the difficult task of correlating the doublets observed in the Mössbauer spectra with the sites available for Fe occupancy in the structure. As discussed earlier, previous workers have been divided on the central issue of assigning the innermost peaks of the spectra to either tetrahedral or octahedral environments. It was hoped that the compositional variation represented by the specimens in this study would provide insight into this issue by producing obvious correlations between major element compositions and site occupancies. Although such clues exist in our data base, their interpretation must

still be made in light of a number of crystal chemical assumptions to be discussed.

Mössbauer doublet 1

The largest doublet in a Mössbauer spectrum of staurolite is universally assigned to the tetrahedral Fe site in the structure and has an *IS* of 0.98 mm/s and a *QS* of 2.45 mm/s. Assignment of this doublet to tetrahedral coordination, and therefore to the Fe site, on the basis of δ and Δ is consistent with parameters observed for Fe^{2+} in the tetrahedral sites in other minerals such as spinels (Bancroft, 1973). However, if this doublet is interpreted as indicating the only Fe site, then its area is anomalously small (representing 0.86–1.90 atoms of Fe per formula unit (pfu) based on 48 O atoms) relative to previous workers' predictions of Fe occupancy of that site that are in the range of two to three atoms (even approaching four atoms in synthetic iron staurolite) pfu (e.g., Smith, 1968; Takéuchi et al., 1972). In part because it is the largest

TABLE 3—*Continued*

ER-70	117183	82TP9	82TP9A	203	HV-4	HV-10	HV-112	HV-116
7.595	7.674	7.529	7.157	7.480	7.616	7.669	7.615	7.666
17.785	17.697	17.788	17.875	17.925	17.597	17.819	17.640	17.561
0.112	0.130	0.095	0.077	0.083	0.116	0.122	0.116	0.127
0.013	0.022	0.000	0.000	0.000	0.000	0.000	0.000	0.000
0.006	0.006	0.000	0.000	0.000	0.000	0.000	0.000	0.000
0.007	0.004	0.000	0.000	0.000	0.000	0.000	0.000	0.000
2.764	2.505	1.499	1.848	2.443	2.737	2.428	2.572	2.692
0.443	0.317	0.185	0.249	0.267	0.364	0.271	0.359	0.401
0.204	0.094	0.147	0.206	0.089	0.197	0.092	0.292	0.233
0.102	0.317	0.055	0.069	0.267	0.098	0.363	0.096	0.100
3.312	3.138	1.740	2.166	2.980	3.198	3.094	3.027	3.201
0.204	0.094	0.147	0.206	0.089	0.197	0.092	0.292	0.233
3.516	3.232	1.887	2.372	3.069	3.395	3.186	3.319	3.425
0.680	0.901	1.032	0.990	0.520	0.769	0.773	0.929	0.856
0.067	0.052	0.453	0.325	0.072	0.026	0.022	0.057	0.021
0.056	0.047	0.814	0.570	0.047	0.049	0.236	0.037	0.043
0.113	0.011	0.224	0.236	0.265	0.280	0.272	0.214	0.158
2.779	3.026	3.398	(3.806)	4.200	3.323	(2.583)	2.964	3.061

FE80	FE70	FE60	FL402	FL404	FL353	LA251	FM222	FL225	LA7672
8.000	8.000	8.000	7.500	7.500	7.500	8.000	7.500	7.500	8.000
18.000	18.000	18.000	18.000	18.000	18.100	17.900	18.000	18.600	17.800
0.000	0.000	0.000	0.000	0.000	0.000	0.000	0.000	0.000	0.000
0.000	0.000	0.000	0.000	0.000	0.000	0.000	0.000	0.000	0.000
0.000	0.000	0.000	0.000	0.000	0.000	0.000	0.000	0.000	0.000
0.000	0.000	0.000	0.000	0.000	0.000	0.000	0.000	0.000	0.000
2.640	2.201	1.934	2.784	3.372	2.916	1.990	1.568	1.613	2.406
0.186	0.328	0.257	0.628	0.352	0.343	0.280	0.078	0.403	0.339
0.279	0.190	0.139	0.472	0.156	0.137	0.153	0.294	0.169	0.168
0.093	0.081	0.070	0.116	0.116	0.102	0.078	0.058	0.063	0.084
2.921	2.610	2.261	3.528	3.844	3.364	2.348	1.706	2.081	2.832
0.279	0.190	0.139	0.472	0.156	0.137	0.153	0.294	0.169	0.168
3.200	2.800	2.400	4.000	4.000	3.500	2.500	2.000	2.250	3.000
0.800	1.200	1.600	0.000	0.000	0.000	0.000	2.000	0.000	0.000
0.000	0.000	0.000	0.000	0.000	0.000	0.000	0.000	0.000	0.000
0.000	0.000	0.000	0.000	0.000	0.000	0.000	0.000	0.000	0.000
0.000	0.000	0.000	0.000	0.000	0.500	1.500	0.000	1.700	1.000

doublet, this site has the smallest standard deviations on its positional parameters, although its area varies over a statistically significant range from 26 to 62% of the total peak area in the spectra.

Mössbauer doublets 2 and 3

Consistency with previous occupancy data based on Mössbauer analyses can be obtained if doublets 2 and 3 of this study, with average parameters of $\delta = 0.98$ and 0.99 mm/s, and $\Delta = 2.10$ and 1.59 mm/s, respectively, are also assigned to Fe^{2+} in the Fe site. Such an interpretation would corroborate the existence of the (at least) three separate centers of displacement around the Fe site first observed by Smith (1968) and later corroborated by Bringhurst and Griffen (1986) and Alexander (1989). However, this model raises some questions. (1) As pointed out by Alexander (1989), the precision of the X-ray structure refinement may be questionable for such closely spaced sites. In fact she suggests that more than three Fe subsites may exist. (2) The interpretation of the Mössbauer data is unclear because doublets 2 and 3 have been shown by previous workers to have temperature depen-

dences that must be explained by tetrahedral Fe subsite occupancy. Also, the Fe subsites may not be sufficiently distinct geometrically to yield three such very distinct Mössbauer doublets with well-defined parameters. In addition, the parameters for doublets 2 and 3 fall into a range that may be interpreted to represent Fe^{2+} in a highly distorted octahedral environment, as discussed above. The question of temperature dependence will not be explicitly treated here. There are many conflicting interpretations, and a careful study involving temperature variations and resolution of five doublets would be required to resolve the question. However, the latter two issues involving the Mössbauer data merit the following discussion for clarification.

How distinct must sites occupied by Fe atoms in a crystal structure be to yield resolvable doublets in a Mössbauer spectrum? This issue has been the subject of extensive debate, particularly for such phases as spinels (Bancroft et al., 1983) and orthopyroxenes (Seifert, 1983). For these phases partial QS (for spinels) and distinct populations of nearest neighbor cations (for orthopyroxenes) have been invoked to explain multiple peaks observed

TABLE 4. Staurolite peak parameters

Sample	Site 1				Site 2				Site 3			
	IS	QS	A	W	IS	QS	A	W	IS	QS	A	W
356-1	0.97	2.44	41	0.30	0.97	2.11	28	0.30	0.96	1.60	12	0.30
EH-6	0.98	2.41	43	0.32	1.00	2.04	21	0.32	0.99	1.43	11	0.32
B14040	0.97	2.47	37	0.28	0.97	2.17	30	0.28	0.97	1.72	13	0.28
117189	0.98	2.38	47	0.31	0.99	2.02	24	0.31	0.99	1.42	12	0.31
6-3	0.98	2.43	48	0.31	0.98	2.12	26	0.31	0.93	1.50	9	0.31
3-3	0.97	2.45	39	0.29	0.97	2.15	29	0.29	0.96	1.67	12	0.29
114-1	0.97	2.43	43	0.32	0.97	2.12	26	0.32	0.95	1.61	11	0.32
53-2	0.97	2.45	38	0.30	0.97	2.15	30	0.30	0.96	1.66	11	0.30
ER-70	0.98	2.39	45	0.31	0.98	2.03	23	0.31	0.97	1.43	13	0.31
117183	0.97	2.45	37	0.29	0.98	2.14	30	0.29	0.98	1.69	12	0.29
82TP9	0.97	2.46	45	0.31	0.97	2.11	24	0.31	0.97	1.54	12	0.31
I2TP9A	0.98	2.43	46	0.31	0.99	2.08	24	0.31	0.97	1.51	11	0.31
203	0.99	2.55	35	0.31	0.98	2.26	34	0.31	1.00	1.84	13	0.31
HV-4	0.98	2.47	30	0.27	0.98	2.16	34	0.33	0.97	1.57	19	0.47
HV-10	0.97	2.44	38	0.29	0.98	2.14	30	0.29	0.97	1.68	12	0.29
HV-112	0.98	2.44	42	0.34	0.96	2.14	26	0.34	0.96	1.50	11	0.34
HV-116	0.98	2.47	26	0.25	0.98	2.16	34	0.31	0.98	1.58	21	0.45
77-55C	0.98	2.44	47	0.32	0.99	2.08	24	0.32	1.00	1.51	11	0.32
71-60E	0.98	2.53	46	0.28	0.98	2.17	23	0.28	1.00	1.74	11	0.28
71-62R	0.98	2.53	46	0.29	0.98	2.18	24	0.29	1.01	1.72	10	0.29
71-62U	0.98	2.53	47	0.29	0.98	2.17	23	0.29	1.00	1.73	11	0.29
71-62T	0.98	2.53	46	0.29	0.98	2.16	23	0.29	1.00	1.72	11	0.29
71-62B	0.98	2.52	46	0.29	0.98	2.16	23	0.29	0.98	1.70	11	0.29
Fe100	0.98	2.35	43	0.40	0.97	2.01	27	0.40	0.95	1.46	13	0.40
Fe90	0.99	2.39	41	0.32	0.98	2.02	28	0.32	0.98	1.55	12	0.32
Fe80	0.99	2.35	50	0.36	0.99	1.91	21	0.36	0.95	1.32	14	0.36
Fe70	0.97	2.46	37	0.32	0.98	2.12	30	0.32	0.97	1.59	14	0.32
Fe60	0.97	2.38	45	0.34	0.98	2.00	24	0.34	0.97	1.46	14	0.34
FeLi-40-2	0.96	2.45	35	0.36	0.99	2.07	23	0.36	0.96	1.57	13	0.36
FeLi-40-4	1.05	2.55	37	0.37	1.03	2.14	36	0.37	0.94	1.84	13	0.37
FeLi-35-3	1.00	2.54	34	0.35	1.00	2.20	37	0.35	0.96	1.76	14	0.35
LiAl-25-1	0.97	2.52	46	0.30	0.97	2.17	24	0.30	0.97	1.69	8	0.30
FeMg-22-2	0.98	2.32	54	0.40	0.97	1.76	18	0.40	1.04	1.02	8	0.40
FeLi-225-1	0.98	2.46	46	0.32	0.99	2.11	27	0.37	—	—	—	—
LiAl-767-2	0.97	2.44	62	0.36	0.97	1.97	20	0.36	—	—	—	—
AVG	0.98	2.44	42	0.32	0.98	2.08	27	0.33	0.97	1.55	13	0.34
STD	0.02	0.05	7	0.04	0.01	0.09	5	0.03	0.02	0.16	3	0.05

Note: IS = isomer shift, *QS* = quadrupole splitting, parameters relative to metallic Fe foil and given in units of mm/s. *A* = % area of doublet relative to Fe$_{tot}$, *W* = width of peaks in mm/s. CHI2 = chi-squared value for fit, %MIS = percent misfit, and %UNC = percent uncertainty, the latter two after the convention of Ruby, 1973. AVG = average of all samples excluding (—); STD = standard deviation. Due to their small size and overlap with adjacent peaks, both doublets 5 and 6 could not be resolved in any one spectrum. Threshold values of 3% of Fe$_{tot}$ can probably be safely assumed for all undetected sites in this table. Calculated formula units given in Table 3 reflect these minimums.

for a single site in Mössbauer spectra. These two mineral groups provide a precedent for assigning multiple doublets to represent subsites of a single crystallographic site in a mineral, such as may be the case in staurolite.

An opposite problem is encountered for most Fe-bearing members of the amphibole group, in which four distinct sites (M1–M4) occupied by Fe are known from crystal structure refinements but in which only two doublets are resolved in Mössbauer analysis (e.g., Hawthorne, 1981a). Why can multiple doublets be resolved for subsets of single sites in some minerals, while in other minerals multiple sites cannot even be resolved?

Hawthorne (1976, 1978) gave a partial answer to this question by applying a method for evaluating the distortion produced by variation in bond lengths and angles for a given site (in amphiboles, in particular). Quantitative estimates of the deviation of a crystallographic site from ideal geometry may be calculated from the bond angles and interatomic distances between a cation and its surrounding O atoms. The resulting parameters are termed angle variance (based on bond angles) and polyhedral distortion (based on bond lengths). For amphiboles, an inverse correlation is observed between the so-called variance and distortion parameters of the M2–M4 sites. These two effects may cancel so that three peaks cannot be resolved. For comparison, we calculated variance and distortion parameters for the three postulated Fe subsites in staurolite based on atomic positions given by Alexander (1989); the results are shown in Table 7. This calculation is at best only an approximation because averaged O positions must be used [rather than the shifts in the O positions undoubtedly present but difficult to resolve by X-ray diffraction (XRD) considering the reduced scattering power of O]. However it does reflect the greater distortion for lesser and lesser occupied subsites. For staurolite, the variance and distortion parameters are positively correlated, strongly implying that the sites may be sufficiently distinct to yield different Mössbauer dou-

TABLE 4—*Continued*

Site 4				Site 5				Site 6				CHI2	%MIS	%UNC
IS	QS	A	W	IS	QS	A	W	IS	QS	A	W			
1.11	0.89	8	0.30	—	—	—	—	0.88	0.93	10	0.30	518	0.002	0.002
1.09	0.63	12	0.32	0.12	0.90	12	0.32	—	—	—	—	530	0.007	0.003
1.10	0.97	10	0.28	—	—	—	—	0.86	1.10	10	0.28	518	0.003	0.002
1.02	0.79	13	0.31	0.08	0.71	4	0.31	—	—	—	—	516	0.004	0.004
1.01	0.75	10	0.31	0.06	0.71	5	0.31	—	—	—	—	534	0.013	0.006
1.09	0.92	10	0.29	—	—	—	—	0.86	0.97	10	0.29	529	0.012	0.006
1.08	0.89	10	0.32	—	—	—	—	0.86	0.91	10	0.32	535	0.010	0.004
1.10	0.91	10	0.30	—	—	—	—	0.86	0.94	10	0.30	522	0.005	0.003
1.06	0.69	13	0.31	0.08	0.80	6	0.31	—	—	—	—	522	0.005	0.003
1.10	0.96	10	0.29	—	—	—	—	0.87	0.97	10	0.29	533	0.009	0.004
1.04	0.73	10	0.31	0.15	0.58	8	0.31	—	—	—	—	520	0.008	0.006
1.06	0.77	11	0.31	0.07	0.77	9	0.31	—	—	—	—	513	0.001	0.008
1.17	0.96	9	0.31	—	—	—	—	0.87	0.92	9	0.31	526	0.013	0.007
1.08	0.70	11	0.35	0.07	0.84	6	0.27	—	—	—	—	527	0.004	0.002
1.10	0.95	10	0.28	—	—	—	—	0.86	0.96	12	0.29	518	0.004	0.003
1.08	0.68	11	0.34	0.25	0.49	9	0.33	—	—	—	—	513	0.001	0.001
1.08	0.85	12	0.35	0.08	0.85	7	0.30	—	—	—	—	518	0.002	0.001
1.09	0.70	11	0.32	0.11	0.90	7	0.32	—	—	—	—	523	0.006	0.004
1.18	0.91	10	0.28	—	—	—	—	0.91	0.89	8	0.28	535	0.013	0.005
1.20	0.87	11	0.29	—	—	—	—	0.95	0.88	9	0.29	526	0.009	0.005
1.19	0.88	10	0.29	—	—	—	—	0.94	0.88	9	0.29	519	0.003	0.002
1.20	0.88	10	0.29	—	—	—	—	0.95	0.88	9	0.29	526	0.006	0.003
1.13	0.84	13	0.29	—	—	—	—	0.85	0.84	7	0.29	522	0.007	0.004
1.05	0.74	10	0.40	0.06	0.80	7	0.30	—	—	—	—	520	0.006	0.006
1.07	0.83	11	0.32	0.06	0.69	8	0.23	—	—	—	—	539	0.063	0.024
1.02	0.53	6	0.36	0.08	0.83	9	0.25	—	—	—	—	547	0.072	0.026
1.04	0.84	12	0.32	0.12	0.51	7	0.32	—	—	—	—	519	0.016	0.012
1.01	0.84	11	0.34	0.09	0.68	6	0.34	—	—	—	—	514	0.003	0.005
1.07	0.76	16	0.36	0.14	0.62	12	0.36	—	—	—	—	527	0.012	0.006
0.98	1.07	9	0.37	0.19	1.17	4	0.37	—	—	—	—	514	0.002	0.005
0.98	1.05	10	0.35	0.22	1.11	4	0.35	—	—	—	—	520	0.016	0.014
1.01	0.83	11	0.30	0.10	0.51	6	0.30	—	—	—	—	516	0.005	0.005
1.06	0.58	4	0.40	0.05	0.64	15	0.40	—	—	—	—	529	0.088	0.049
0.91	1.11	19	0.47	0.09	1.05	8	0.27	—	—	—	—	601	0.115	0.024
0.96	1.09	12	0.36	0.14	1.20	6	0.36	—	—	—	—	539	0.039	0.015
1.05	0.83	11	0.33	0.11	0.79	8	0.32	0.89	0.93	9	0.29	527	0.019	0.009
0.05	0.15	3	0.04	0.05	0.20	3	0.04	0.04	0.06	1	0.01	17	0.029	0.010

blets. In other words, the electric field gradient at each of the Fe atoms in the three Fe subsites differs significantly. The reasons for such variance are discussed below.

Assignment of doublets 1, 2, and 3 to the three subsites of Fe is consistent with the substitutions represented by the compositional variation in our data. For example, consider the Fe site occupancies of synthetic samples with variable Fe-Mg ratios (Fig. 6). In the Fe100 synthetic sample with 100% Fe and no Mg, occupancies of the three Fe subsites are 1.7, 1.1, and 0.5 formula units (corresponding to doublets 1, 2, and 3, respectively). If it is assumed that Mg substitutes mainly into the Fe site as proposed by Holdaway et al. (1986b) and Alexander (1989), then as Mg content increases, Fe content decreases concomitantly in doublets 1, 2, and 3 as long as these sites all represent subsites of Fe. Indeed, as Mg increases the percentage of Fe_{tot} in each site remains relatively constant, but the number of formula units of Fe in each Fe subsite decreases proportionally. For sample Fe60, formula units of Fe in doublet 1 decrease to 1.1, which is 65% of 1.7. Doublet 2 and 3 occupancies decrease to 0.6 and 0.3 or 54% and 60% of their original contents. Thus there is a good correlation between the addition of Mg to

the Fe site and the proportional reduction of Fe^{2+} occupancy in doublets 1, 2, and 3. Although this point should not be overstated owing to considerable noise in the data (attributable to large errors in the spectra of the synthetic staurolite samples as discussed above), there is no question that the total Fe in doublets 1, 2, and 3 decreases as Mg is added. Such a variation would be likely if doublets 1, 2, and 3 represent the three subsites of the tetrahedral Fe site. Fe and Mg apparently have similar preferences for partitioning among the three subsites, as might be expected for cations of identical charge and similar size.

Which Mössbauer doublets correspond to which of the three Fe subsites? Alexander (1989) makes the following assignments based on the peak areas of her Mössbauer spectra and on subsite occupancies determined by XRD data:

ΔRT (mm/s)	% Area	Assignment	Other occupied sites
2.50	23	Fe2	P(1A) Al(3B)
2.13	40	Fe1	Al(3A) Al(3B)
1.17	31	Fe3	P(1B) Al(3A)

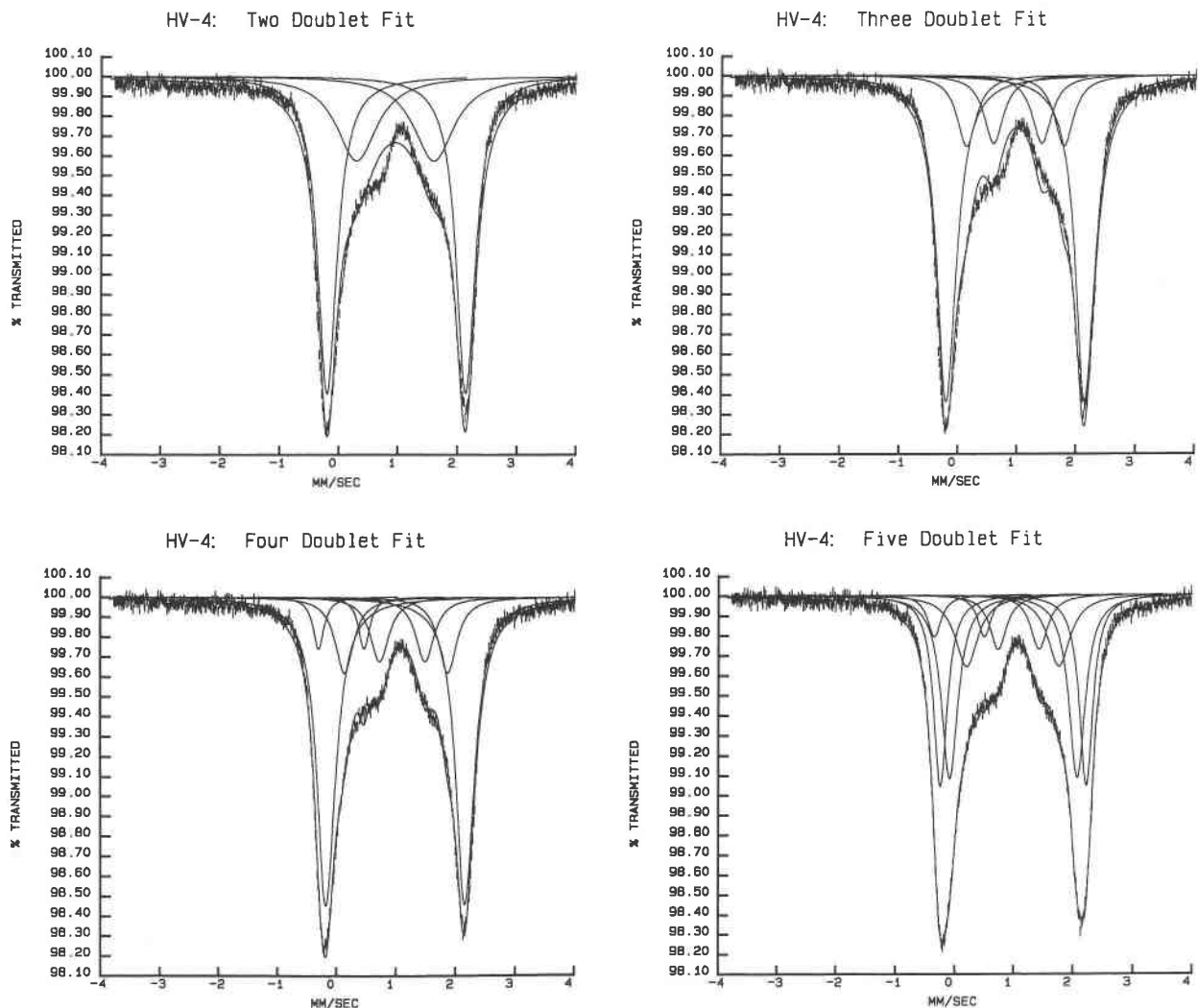Fe3 is expected to be more occupied than Fe2 because

Fig. 2. Mössbauer spectra of Hunt Valley sample HV-4 showing improvement of model with the addition of doublets to the fits. Parameters of these fits are given in Table 5.

Fe3 is associated with occupancy of P(1B) [and P(1B) is in turn related to the occupancy of Al(3A)]. Al(3A) is usually more occupied than Al(3B), and thus, P(1B) should be more occupied than P(1A).

Using the same reasoning and average Mössbauer parameter values, we obtain different assignments for the doublets. Moreover, our assignments are also supported by geometrical considerations. It is well known (e.g., Bancroft, 1973) that quadrupole splitting values respond to the type of environment in which an Fe atom resides. For Fe^{2+}, large Δ values are associated with regular, undistorted coordination polyhedra, with increasingly greater amounts of distortion represented by decreasing Δ values. If this information is coupled with the distortion parameters calculated according to Hawthorne's (1978, 1981b) method (Table 7) and based on Alexander's (1989) subsite positional parameters, we obtain the following assignments:

ΔRT (mm/s)	% Area	Distortion	Assignment	Other occupied sites
2.45	43	most regular	Fe1	Al(3A) Al(3B)
2.10	27	intermediate	Fe3	P(1B) Al(3A)
1.59	12	most distorted	Fe2	P(1A) Al(3B)

In general, assignment of the subsites on the basis of distortion parameters and the interpretation of the QS brings our data into agreement with Alexander's (1989) predictions of subsite occupancies based on relative occupancies of Al(3A) and Al(3B).

Our assignments are also supported by the data from the Li-Fe staurolite samples studied here (Fig. 7). Although the quality of some of our data suffers from small sample sizes, our results show that the areas of the Fe2 and Fe3 doublets decrease as Li content increases, whereas the area of the Fe1 doublet decreases only slightly. Li^{1+} substitution is primarily controlled by Al (see Dutrow,
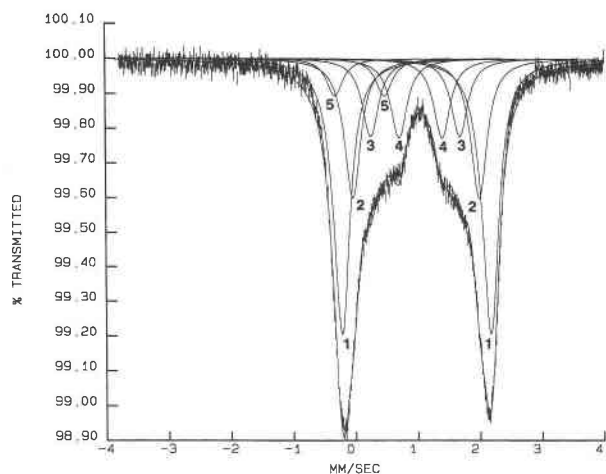
TABLE 5. HV-4 successive fits

Number of peaks	Two	Three	Four	Five
CHI2	2935	2432	1142	527
%MIS	0.639	0.522	0.173	0.004
%UNC	0.261	0.024	0.014	0.002
IS 1	0.97	0.97	0.98	0.98
QS 1	2.33	2.34	2.33	2.47
A 1	64	70	64	29
W 1	0.39	0.40	0.38	0.27
IS 2	0.95	0.96	0.99	0.98
QS 2	1.29	1.64	1.73	2.16
A 2	36	15	16	34
W 2	0.83	0.40	0.38	0.33
IS 3	—	1.00	1.09	0.97
QS 3	—	0.81	0.76	1.57
A 3	—	15	14	19
W 3	—	0.40	0.38	0.47
IS 4	—	—	0.07	1.08
QS 4	—	—	0.77	0.70
A 4	—	—	6	11
W 4	—	—	0.22	0.35
IS 5	—	—	—	0.07
QS 5	—	—	—	0.84
A 5	—	—	—	6
W 5	—	—	—	0.27

Note: See footnote in Table 4 for abbreviations.

Fig. 3. Mössbauer spectrum of staurolite no. 117183 from Fannin County, Georgia from the collection of the Smithsonian Institution (Holdaway et al., 1986b). The spectrum of this sample contains no Fe^{3+} doublet. The proportion of Fe^{2+} in the Fe sites is in the ratio 37/30/12 for Fe1, Fe2, and Fe3, respectively.

1991); however, that substitution is coupled to vacancies by the relationship $Li^{1+} + \frac{1}{3} \square = \frac{1}{3} Al + 1 \square$. Therefore the increasing Li content in our samples causes increased Al occupancy in the Al(3) sites, which then reduces H^+ occupancy in the P(1) sites. The Al(3) and adjacent P(1) sites are not expected to be simultaneously occupied because they are so close together (Fig. 1). Occupancy of the P(1) sites is by definition associated with Fe occupan-

TABLE 6. Estimated errors for Mössbauer parameters (after Dollase, 1975)

Percent errors in parameters assuming isolated peaks							
Natural sample 71-62T (best case)				Synthetic sample Fe-80 (worst case)			
	Position	Area	Width		Position	Area	Width
Site 1	0.3	0.6	0.8	Site 1	0.8	1.6	2.2
Site 2	0.4	0.7	1.0	Site 2	1.5	3.0	4.1
Site 3	0.5	1.0	1.3	Site 3	2.9	5.8	8.0
Site 4	0.6	1.2	1.6	Site 4	6.8	13.5	18.6
Site 6	1.3	2.6	3.5	Site 5	3.9	7.8	10.6

Percent errors in peak areas due to overlap									
Natural sample 71-62T									
Peak position	235	250	282	298	361	345	378	391	401
227	1.2	0.5	0.5	0.6	0.6	0.5	0.4	0.4	0.3
235		0.8	0.5	0.6	0.6	0.5	0.5	0.4	0.4
250			0.6	0.8	0.8	0.6	0.5	0.5	0.4
282				1.2	0.9	0.7	0.6	0.5	0.5
298					1.4	0.9	0.8	0.6	0.6
361						1.2	1.0	0.7	0.6
345							0.3	0.5	0.5
378								0.9	0.5
391									1.0
Synthetic sample Fe-80									
Peak position	245	264	223	291	343	276	360	381	395
232	2.3	1.4	5.4	1.5	1.5	1.6	1.4	1.2	0.9
245		2.7	3.0	2.4	2.4	2.7	2.2	1.6	1.2
264			4.5	3.7	3.7	4.5	3.2	2.2	1.4
223				5.5	5.5	7.5	4.5	2.7	1.6
291					4.3	8.5	3.7	2.4	1.5
343						5.5	4.7	2.4	1.5
276							4.5	2.7	1.6
360								2.3	1.4
381									1.7

Fig. 4. Mössbauer spectrum of sample ER-70 from the Errol quadrangle, New Hampshire (Holdaway et al., 1986b). A total of 6% of the Fe in this sample is Fe^{3+}.

cy in the Fe2 or Fe3 sites, so it is not unexpected that Fe occupancy in Fe2 and Fe3 decreases with increasing Li.

Ståhl et al. (1988) use a different terminology for the two Mössbauer doublets which they assign to four of six structural domains. The largest doublet relates to concurrent occupancy of their H(1) [equivalent to P(1)] and one of the Al(3) sites, and the smaller doublet corresponds to occupation of only Al(3A) or Al(3B). Therefore, Ståhl et al. (1988) agree that the presence of protons affects the Fe subsite occupancies, but correlate the most occupied site with the presence of H [Alexander's (1989) Fe2 and Fe3]. It may be that resolution of their H(2) site decreased the observed electron density at the Fe1 site.

Our data do not support the interpretation that doublets 2 and 3 are octahedrally coordinated for the following reasons. (1) If these doublets represent occupancies of
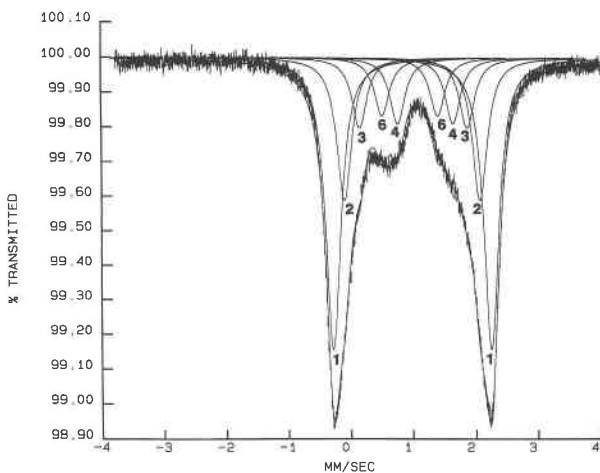
Fig. 5. Mössbauer spectrum of sample 71-62T from Black Mountain, New Hampshire (Rumble, 1978). This spectrum contains no Fe^{3+} doublet, yet its spectral profile is subtly different from that in Figure 3 because of different occupancies of the Fe site in the ratio 46/23/11 for Fe1, Fe2, and Fe3.

TABLE 7. Parameters for staurolite sites

		Distortion parameters (after Hawthorne, 1981a):				
			Variance			Distortion
Fe1	O1A-O1B	110.22		Fe1-O1A	1.980	
	O1A-O5	109.27		Fe1-O1B	1.966	
	O1B-O5	109.43		Fe1-O5	2.026	
	O5-O5	109.21	0.1438	mean	2.000	1.7994
Fe2	O1A-O1B	101.09		Fe2-O1A	2.225	
	O1A-O5	103.54		Fe2-O1B	1.961	
	O1B-O5	113.90		Fe2-O5	1.927	
	O5-O5	118.00	50.4706	mean	2.010	38.7685
Fe3	O1A-O1B	102.33		Fe3-O1A	1.992	
	O1A-O5	112.55		Fe3-O1B	2.161	
	O1B-O5	105.28		Fe3-O5	1.936	
	O5-O5	117.13	32.723	mean	2.006	21.211
Si	O2A-O2B	108.53		Si-O2A	1.638	
	O2A-O3	108.95		Si-O2B	1.632	
	O2A-O4	111.24		Si-O3	1.653	
	O2B-O3	109.35		Si-O4	1.637	
	O2B-O4	110.57		mean	1.640	0.2212
	O3-O4	108.16	1.4442			

	Atomic coordinates:		
	x	y	z
Fe1	0.3778	0.0000	0.2497
Fe2	0.4027	0.0000	0.2783
Fe3	0.3994	0.0000	0.2291
Fe	0.3897	0.0000	0.2471
Si	0.1342	0.1662	0.2482
O1A	0.2328	0.0000	−0.0372
O1B	0.2358	0.0000	0.5339
O5	0.5270	0.0996	0.2495
O2A	0.2558	0.1614	0.0152
O2B	0.2545	0.1610	0.4835
O3	0.0015	0.0889	0.2447
O4	0.0218	0.2493	0.2493

extremely distorted octahedral sites, presumably U1, U2, Al(3A), and Al(3B) as suggested by previous workers, we would expect the parameters to be sensitive to changes in composition, particularly over the extremes represented in our data. Our data uniformly display nearly constant IS and QS (standard deviations of 0.01 and 0.02 mm/s for δ and 0.09 and 0.16 mm/s for Δ on doublets 2 and 3). (2) Although the octahedral ferrous doublets in ilvaite as reported by Nolet and Burns (1979) (IS = 1.05, 0.99 mm/s; QS = 2.46, 2.26 mm/s) correspond quite well with doublets 1 and 2, assignment of both these sites to octahedral coordination would result in approximately 70% of the Fe in sixfold coordination. This large amount is in conflict with the results of X-ray structure refinements. Therefore, we do not interpret any of the Fe subsite doublets to represent an octahedral site.

Mössbauer doublet 4

The one doublet observed in our Mössbauer data which unequivocally corresponds to Fe in octahedral coordination is that labeled doublet 4. Its mean parameters of δ = 1.07 mm/s and Δ = 0.84 mm/s are well within a range conventionally assigned to Fe^{2+} in octahedral coordination (Bancroft, 1973), and the low QS implies occupancy in a very distorted site. In staurolite the site represented by this doublet must be either Al(3A), Al(3B), U(1), U(2), or some unresolvable combination of them. Large error bars for this doublet, resulting from the fact
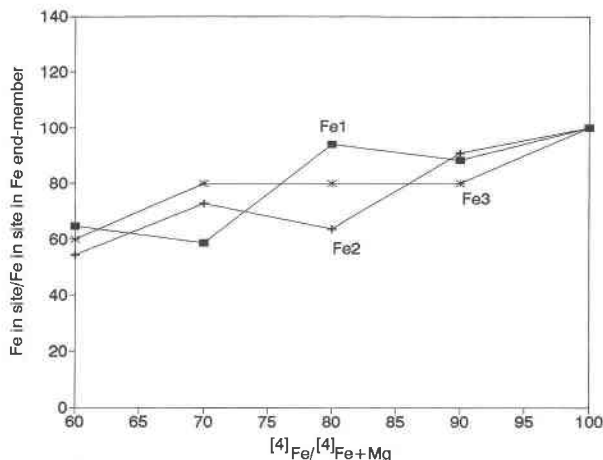
Fig. 6. Decreasing occupancies in the Fe subsites with increasing Mg contents based on data for the Fe-Mg synthetic staurolite samples. Note that Mg appears to displace Fe^{2+} from all three subsites proportionately, suggesting that Mg has site preferences identical to those of Fe^{2+} for this site. Scale is equivalent to Figure 7 to facilitate comparison.
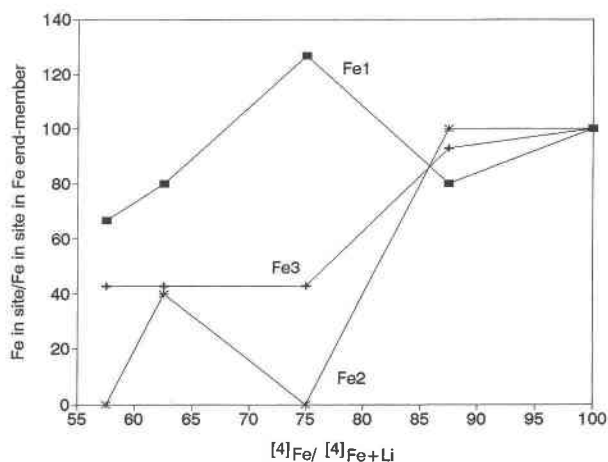
Fig. 7. Fe occupancies in the Fe subsites as a function of increasing Li substitution, based on the synthetic Fe-Li staurolite samples. Fe1 occupancy by Fe^{2+} does not appear to vary significantly as Li^{1+} is introduced; however, Fe2 and Fe3 occupancies by Fe^{2+} decrease. This suggests that Li^{1+} has a site preference for the Fe2 and Fe3 sites which are associated with occupied P(1A) or P(1B) H positions.

that it is relatively small and overlapped by adjacent peaks, make impossible any correlation with compositional data in a direct way. This peak also has the largest standard deviation of its *IS*. This observation implies (1) that $^{[6]}Fe^{2+}$ does not confine itself to any particular octahedral site, (2) that the octahedral site is responding to next nearest neighbor effects, or (3) that resolution of this doublet is exceedingly difficult because of its position in the spectrum. In any case, Mössbauer data alone cannot be used to confirm any preference for any particular octahedral site in the staurolite structure.

Even with the aid of occupancy data from structure refinements, it is difficult to place constraints on the interpretation of the Mössbauer data for doublet 4. The doublet represents between 0.19 and 0.6 Fe^{2+} atoms pfu. Although neutron diffraction and X-ray data collected by different workers suggest different occupancies for the Al(3A), Al(3B), U(1), and U(2) sites (e.g., Ståhl et al., 1988; Alexander, 1989), they generally predict that the total Fe occupancy of the U(1) and U(2) sites combined is no greater than the 10% value suggested by Holdaway et al. (1986b), for U(1), which corresponds to 0.20 Fe pfu. The structure refinements, however, represent a population of only six samples, in contrast with the 35 studied here. Therefore, it is likely that not all of the octahedral Fe^{2+} can be assigned to U(1) and U(2); in some samples, some of the octahedral Fe^{2+} must be in Al(3A), or Al(3B), or both. Beyond that conclusion the Mössbauer data cannot be brought to bear on the issue of whether or not the octahedral Fe^{2+} is confined to Al(3A) or Al(3B) (or both). Given the lack of consensus among structure refinements on this issue it seems likely that cation occupancies among the Al(3A), Al(3B), U(1) and U(2) sites may be widely variable in response to substitutions of various cations in the nearby Fe site.

Mössbauer doublet 5

The Mössbauer parameters for doublet 5 average 0.10 mm/s with a standard deviation of 0.04 mm/s for δ, and 0.77 mm/s with a standard deviation of 0.20 for Δ. These values are similar to those found by Varma and Varma (1987) and Sharma et al. (1987; see Table 1) although they interpreted the doublet as $^{[6]}Fe^{3+}$ and Fe^{3+} in an impurity, respectively. They do not agree with parameters reported by Alexander (1989), but as noted above, the reported parameters would appear to be in error based on her published spectrum. The values reported in the present study are typical of Fe^{3+} in tetrahedral coordination, indicating in this case that Fe^{3+} is either in the Fe site or in the Si site.

All of the synthetic samples in this study contain Fe^{3+} regardless of the conditions of synthesis. A baseline of 3–9% of Fe_{tot} as Fe^{3+} is exceeded only in samples synthesized under conditions of the FMQ buffer used for sample FM222, which has 15% of Fe_{tot} as Fe^{3+}. The presence of Fe^{3+} may be controlled by some combination of structural constraints and f_{O_2}, or it may be related to the high pressures used in the syntheses.

Unfortunately, Mössbauer parameters of the Fe^{3+} doublets do not yield any clues that might decisively indicate the occupancy of either the Fe subsite or the Si site. *QS* in the observed range suggest an environment that is neither highly distorted nor extremely regular (for Fe^{3+}, high Δ implies increasing distortion—the opposite of the trend for Fe^{2+}; see Dyar, 1984). It is difficult to equate doublet 5 to any of the Fe^{2+} doublets on the basis of *IS*, but it can be tentatively equated to either Fe2 or Fe3 based on *QS*. This assignment is not entirely satisfactory, however, because of the presence of H atoms in nearby sites. Both the Fe2 and the Fe3 subsites are associated with occupied

P1 sites, while the Fe1 subsite is not. If Fe^{3+} occupies any of the Fe subsites, it is expected to avoid H^+ and therefore display a preference for Fe1. Therefore, Fe^{3+} occupancy in the Fe site is difficult to reconcile with our Mössbauer data.

The assignment of Fe^{3+} to the Si site is suggested by the neutron scattering data of Tagai and Joswig (1985). Therefore, as shown in Table 7, variance and distortion parameters have also been calculated for the Si site; they are roughly the same as those of the Fe1 subsite. However, these parameters are based on Si occupancy of the Si site. If the much larger Fe^{3+} cation occupies the Si site, it would probably introduce a significant amount of local distortion to the site. The observed QS for doublet 5, representative of a somewhat distorted site, would then be expected. That Al^{3+} is known to replace Si in the Si site implies that the substitution of a larger cation in that position is feasible.

We cannot use the Mössbauer data to conclusively rule out the possibility of small amounts (roughly 3% or less of Fe_{tot}) of Fe^{3+} in all samples. All staurolite probably has some small amount of Fe^{3+} hidden in both doublets 5 and 6, but only the larger of these two doublets is resolvable in any given Mössbauer spectrum. It is frustrating that we were unable to resolve all six doublets in our spectra; however, the errors for the extremely small doublets 5 and 6 (if they could both be resolved) would probably be too large for the results to be statistically significant. For this reason we have tentatively assigned 3% occupancy to all sites for which doublets were not resolved (i.e., doublets 5 and 6), and these occupancies are reflected in Table 3.

Mössbauer doublet 6

Doublet 6 is the most difficult of the doublets in our spectra to interpret. Its Mössbauer parameters, $\delta = 0.89$ mm/s and $\Delta = 0.93$ mm/s, place it in the extremely low end of the range for tetrahedral Fe^{2+} in very distorted sites. This doublet could be interpreted in one of three ways: (1) as yet another subsite of the Fe site, (2) as Fe^{2+} in the Si site of the kyanite layer, or (3) as a representative of some type of charge transfer phenomenon.

The first possibility, the occupancy of an additional Fe subsite, is supported by Alexander's (1989) X-ray structure refinement data that show the presence of other minor occupied positions in the Fe tetrahedron. Moreover, the inability to resolve doublet 6 in any of the synthetic samples suggests that the substitutions and nearest-neighbor effects of minor constituents present in natural samples may enhance the distinction of this subsite. However, the occupancy of doublet 6, which ranges from 0.2 to 0.35 cations of Fe^{2+} pfu, represents too many cations for such minor positions, so the possible effects of minor elements can be ruled out. On the basis of dissimilar size and charge, the substitution of the large Fe^{2+} cation for a small Si^{4+} cation in the kyanite sheet is also improbable.

Charge transfer phenomena are also possible in the staurolite structure. Scorzelli et al. (1976) interpreted a doublet in their staurolite spectra with parameters of $\delta = 0.94$ mm/s and $\Delta = 1.25$ mm/s as representing delocalization of electrons between anion vacancies [as suggested by the substitution of Fe^{2+} in the Al(3) sites] and Fe^{2+} in Fe sites. The parameters of our doublet 6 are not far removed from those of Scorzelli et al. (1976), and their hypothesis cannot be ruled out without better Mössbauer spectra and better resolution over a wide temperature range. Charge transfer between metal ions might also be responsible for doublet 6. Although Ward (1984) demonstrated that Fe^{2+}-Ti^{4+} charge transfer between adjacent Fe sites is largely responsible for the color of staurolite, he did not rule out (or even consider) the possibility of Fe^{2+}-Fe^{3+} charge transfer. An electron delocalized (ED) Fe cation would be detected in our Mössbauer spectra if the electrons transfer between sites more rapidly than the lifetime of the Mössbauer transition (10^{-7} s) between the 14.4 keV ground and excited nuclear energy levels of ^{57}Fe. In silicates where an Fe^{2+}-Fe^{3+} ED doublet is detected in Mössbauer spectra, its parameters are in the range of $\delta = 0.67$–0.76 mm/s and $\Delta = 1.36$–1.70 mm/s [e.g., as observed in ilvaite by Nolet and Burns (1979)]. These parameters are different than those observed for our doublet 6, but not so different as to rule out the possible occurrence of Fe^{2+}-Fe^{3+} ED. The synthetic samples, all Ti-free, are varying shades of off-white to tan in color, possibly caused by Fe^{2+}-Fe^{3+} ED or to weak crystal field transitions. Therefore, our data can neither support nor refute the possible interpretation of doublet 6 as a representative of either vacancy-metal or metal-metal charge transfer.

CONCLUSIONS

1. The Mössbauer doublets 1, 2, and 3 represent subsites of the tetrahedral Fe site. Positional disorder of Fe in staurolite based on these subsites seems to be a general trait given the compositional range considered in this study. Subsites are not a result of next nearest neighbor effects as suggested by Ståhl et al. (1988), other than H, because they exist even for the 100% Fe synthetic staurolite.

2. The presence of Mg and Li in the Fe site is supported by the proportional changes in the intensity of the Fe site doublets in the synthetic solid solution series.

3. Doublet 4 represents octahedral Fe^{2+} which may occupy any of the Al(3A), Al(3B), U(1), or U(2) sites.

4. Doublet 5 represents tetrahedral Fe^{3+} in either the Fe or Si sites, but most likely replacing Al in the Si sites.

5. Doublet 6 probably represents Fe occupancy in a charge transfer site.

6. Mössbauer parameters (IS and QS) do not vary systematically with composition.

7. The percentage of Fe in the Fe site is about the same as previously reported ($\sim$80%); however, resolution of more doublets has decreased the observed peak widths and altered the quadrupole splittings of the tetrahedral Fe^{2+} doublets relative to other studies.

8. A study of the temperature dependence of staurolite spectra, in which five doublets are resolved consistently, is needed in order to confirm changes in doublet 2 and 3

occupancies with temperature and to determine if such changes result in overlap of peaks or their disappearance.

REFERENCES CITED

Alexander, V.D. (1989) Iron distribution in staurolite at room and low temperatures. American Mineralogist, 74, 610–619.

Bancroft, G.M. (1973) Mössbauer spectroscopy. Halsted Press, New York.

Bancroft, G.M., Maddock, A.G., and Burns, R.G. (1967) Applications of the Mössbauer effect to silicate mineralogy. I. Iron silicates of known crystal structure. Geochimica et Cosmochimica Acta, 31, 2219–2246.

Bancroft, G.M., Osborne, M.D., and Fleet, M.E. (1983) Next-nearest neighbor effects in the Mössbauer spectra of Cr-spinels: And application of partial quadrupole splittings. Solid State Communications, 47(8), 623–625.

Bringhurst, K.N., and Griffen, D.T. (1986) Staurolite-lusakite series. II. Crystal structure and optical properties of a cobaltoan staurolite. American Mineralogist, 71, 1466–1472.

Dollase, W.L. (1975) Statistical limitations of Mössbauer spectral fitting. American Mineralogist, 60, 257–264.

Donnay, J.D.H., and Donnay, G. (1983) The staurolite story. Tschermaks Mineralogische und Petrographische Mitteilungen, 31, 1–15.

Dowty, E. (1972) Site distribution of iron in staurolite. Earth and Planetary Science Letters, 15, 72–74.

Dutrow, B.L. (1991) The effects of Al and vacancies on Li substitution in iron staurolite: A synthesis approach. American Mineralogist, 76, 42–48.

Dutrow, B.L., Holdaway, M.J., and Hinton, R.W. (1986) Lithium in staurolites and its petrologic significance. Contributions to Mineralogy and Petrology, 94, 496–506.

Dyar, M.D. (1984) Precision and interlaboratory reproducibility of measurements of the Mössbauer effect in minerals. American Mineralogist, 69, 1127–1144.

Dyar, M.D., McGuire, A.V., and Ziegler, R.D. (1989) Redox equilibria and crystal chemistry of coexisting minerals from spinel lherzolite mantle xenoliths. American Mineralogist, 74, 969–980.

Dzhemai, A.Kh. (1978a) Thermal and volume effects and the kinetics of reactions of intraphase distribution of cations. Staurolites. In V.A. Glebovitskii, Ed., Raspred Kationov Termodin Zheleo-Magnez Tverd Rastvorov Silik, p. 173–176. Izd Nauka, Leningrad Old, Leningrad.

——— (1978b) Distribution of cations in structures of iron magnesia silicates. Staurolites. In V.A. Glebovitskii, Ed., Raspred Kationov Termodin Zhelezo-Magnez Tverd Rastvorov Silik, p. 136–152. Izd Nauka, Leningrad Old, Leningrad.

Gibb, T.C. (1968) Estimation of ligand field parameters from Mössbauer spectra. Journal of the Chemical Society (London), A, 1439–1444.

Green, J.C. (1963) High-level metamorphism of pelitic rocks in northern New Hampshire. American Mineralogist, 48, 991–1023.

Griffen, D.T., and Ribbe, P.H. (1973) The crystal chemistry of staurolite. American Journal of Science, 273-A, 479–495.

Hawthorne, F.C. (1976) The crystal chemistry of the amphiboles. V. The structure and chemistry of arfvedsonite. Canadian Mineralogist, 14, 346–356.

——— (1978) The crystal chemistry of the amphiboles. VI. The stereochemistry of the octahedral strip. Canadian Mineralogist, 16, 37–52.

——— (1981a) Crystal chemistry of the amphiboles. Mineralogical Society of America Reviews in Mineralogy, 9A, 1–102.

——— (1981b) Amphibole spectroscopy. Mineralogical Society of America Reviews in Mineralogy, 9A, 103–140.

Holdaway, M.J., Dutrow, B.L., Borthwick, J., Shore, P., Harmon, R.S., and Hinton, R.W. (1986a) H content of staurolite as determined by H extraction line and ion microprobe. American Mineralogist, 71, 1135–1141.

Holdaway, M.J., Dutrow, B.L., and Shore, P. (1986b) A model for the crystal chemistry of staurolite. American Mineralogist, 71, 1142–1159.

Hurst, V.J., Donnay, J.D.H., and Donnay, G. (1956) Staurolite twinning. Mineralogical Magazine, 31, 145–165.

Lang, H.M. (1986) Within outcrop variations in metamorphic conditions, Fetters Schist, Maryland. Geological Society of America Abstracts with Programs, 18, 28.

Náray-Szabó, I. (1929) The structure of staurolite. Zeitschrift für Kristallographie, 71, 103–116.

Nolet, D.A., and Burns, R.G. (1979) Ilvaite: A study of temperature dependent electron delocalization by the Mössbauer effect. Physics and Chemistry of Minerals, 4, 221–234.

Osberg, P.H. (1971) An equilibrium model for buchan-type metamorphic rocks, south-central Maine. American Mineralogist, 56, 570–586.

Phillips, L.V., and Griffen, D.T. (1986) Staurolite-lusakite series. I. Synthetic Fe-Co staurolites. American Mineralogist, 71, 1461–1465.

Regnard, J.R. (1976) Mössbauer study of natural crystals of staurolite. Journal de Physique, Colloque, 37, C6-797–C6-800.

Rice, J.M. (1985) Experimental partitioning of Fe and Mg between coexisting staurolite and garnet. Eos, 66, 1127.

Ruby, S.L. (1973) Why misfit when you already have χ^2? In I.J. Gruverman and C.W. Shenoy, Eds., Mössbauer effect methodology 8, p. 263–276. Plenum Press, New York.

Rumble, Douglas III (1978) Mineralogy, petrology, and isotope geochemistry of the Clough Formation, Black Mountain, western New Hampshire, U.S.A. Journal of Petrology, 19, 317–340.

Scorzelli, R.B., Baggio-Saitovitch, E., and Danon, J. (1976) Mössbauer spectra and electron exchange in tourmaline and staurolite. Journal de Physique, Colloque, 37, C6-801–C6-805.

Seifert, F. (1983) Mössbauer line broadening in aluminous orthopyroxenes: Evidence for next nearest neighbors interactions and short-range order. Neues Jahrbuch für Mineralogie Abhandlungen, 148, 141–162.

Sharma, A.L., Johnson, C.E., McGettigan, T., Jones, D.H., and Thomas, M.F. (1987) On the structure of staurolite through Mössbauer spectroscopy. Hyperfine Interactions, 35, 871–874.

Smith, J.V. (1968) The crystal structure of staurolite. American Mineralogist, 53, 1139–1155.

Stähl, K., Kvick, Å., and Smith, J.V. (1988) A neutron diffraction study of hydrogen positions at 13 K, domain model, and chemical composition of staurolite. Journal of Solid State Chemistry, 73, 362–380.

Stone, A.J., Parkin, K.A., and Dyar, M.D. (1984) Stone: A curve-fitting program for Mössbauer spectra. DEC User's Society Publication 11-720, Marlboro, Massachusetts.

Tagai, T., and Joswig, W. (1985) Untersuchungen der Kationenverteilung im Staurolith durch Neutronenbeugung bei 100 K. Neues Jahrbuch für Mineralogie Monatshefte, 97–107.

Takéuchi, Y., Aikawa, N., and Yamamato, T. (1972) The hydrogen locations and chemical composition of staurolite. Zeitshcrift für Kristallographie, 136, 1–22.

Varma, H.V., and Varma, J. (1987) Mössbauer study of natural staurolite crystals. Journal of Physics, 29, 517–521.

Ward, C.M. (1984) Titanium and the color of staurolite. American Mineralogist, 69, 541–545.

Zen, E-an (1981) Metamorphic mineral assemblages of slightly calcic pelitic rocks in and around the Taconic allochthon, southwestern Massachusetts and adjacent Connecticut and New York. U.S. Geological Survey Professional Paper 1113.